X-ray Absorption Studies on Catechol 2,3-Dioxygenase from *Pseudomonas putida* mt2

Ivano Bertini,‡ Fabrizio Briganti,‡ Stefano Mangani,§ Hans F. Nolting,∥ and Andrea Scozzafava*,‡

Dipartimento di Chimica, Università di Firenze, Via Gino Capponi, 7 I-50121 Firenze, Italy, Dipartimento di Chimica, Università di Siena, Pian dei Mantellini, 44 I-53100 Siena, Italy, and EMBL Outstation, DESY, Notkestrasse, 85 W-2000 Hamburg 52, Germany

Received March 14, 1994; Revised Manuscript Received May 20, 1994®

ABSTRACT: X-ray absorption spectroscopy has been utilized to investigate the structure of the active site of iron(II) catechol 2,3-dioxygenase from *Pseudomonas putida* mt2 both in the native and the 2-chlorophenol inhibited forms. XANES (X-ray absorption near edge structure) and EXAFS (extended X-ray absorption fine structure) results allow us to discuss the coordination number and geometry of the ferrous ion in the native enzyme. The metal geometry is not significantly affected by the binding of the inhibitor. The EXAFS spectrum is consistent with an iron(II) bound to six N/O atoms at an average distance of 2.05 Å or to five N/O at an average distance of 2.04 Å. The simulation of the experimental data is greatly enhanced by considering the iron ligands divided in two different shells. Analysis of the outer shells performed using multiple scattering theory shows that there are histidines in the coordination sphere. The best fitting is obtained assuming the presence of two of them. Similar results are obtained for the inhibited enzyme, which, however, are indicative of a slight shortening of the average metal–donor bond distances. The direct binding of inhibitors to the metal center is confirmed by ^{1}H NMR data.

The catechol dioxygenases are enzymes present in many biological systems involved in the biodegradation of environmental aromatic compounds (Que, 1989; Lipscomb & Orville, 1992; Harayama & Timmis, 1992). They catalyze the oxidation of such compounds through the incorporation of molecular oxygen into the aromatic ring of catechols followed by the ring opening reaction. Depending on the position of the ring breaking the catechol dioxygenases are divided into intradiol and extradiol enzymes. The intradiol dioxygenases usually contain a catalytic high-spin iron(III) ion in the active site. Many investigations have been performed on such systems through biochemical, spectroscopic, and structural studies (Que, 1989). The extradiol enzymes although more abundant than the intradiol enzymes are less stable because of their sensitivity to oxidizing compounds. They usually contain a catalytic high-spin iron(II) ion, difficult to study through electronic spectroscopies (Nozaki et al., 1968). Little is known on the structure and the catalytic mechanism although such enzymes were discovered and isolated about 30 years ago (Kojima et al., 1961).

The catechol 2,3-dioxygenase from *Pseudomonas putida* mt2 first purified and crystallized by Nozaki et al. (1963) is an enzyme containing one high-spin Fe(II) ion for each of the four identical 32 000 MW subunits composing the holoenzyme. The catechol 2,3-dioxygenase enzyme catalyzes the conversion of catechol to α-hydroxymuconic ϵ-semialdehyde as shown in Scheme 1.

Steady-state kinetic studies indicated an ordered bimolecular reaction mechanism with catechol binding first followed by the oxygen molecule (Hori et al., 1973).

The active site has been monitored through EPR active NO derivatives (Arciero et al., 1983, 1985; Arciero & Lipscomb 1986) and through CD, MCD, and electronic absorption spectroscopies (Hirata et al., 1971; Mabrouk et al., 1991). From these studies a pentacoordinated square-pyramidal geometry has been suggested for the iron. Catechol substrates appear to bind the metal ion as bidentate, occupying the axial and one of the equatorial positions of the coordination polyhedron and displacing at least one water molecule. There is also evidence that the oxygen molecule is directly coordinated to the metal ion (Arciero et al., 1985).

Scheme 1

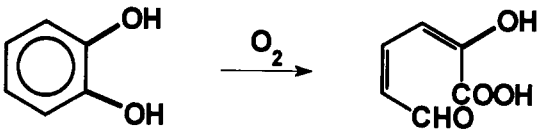

Recently, we have investigated through NMR techniques the interaction of this enzyme with a series of *ortho*-substituted phenols and aliphatic ketones; we have shown that these compounds can coordinate directly to the iron(II) center (Bertini et al., 1994)

The nature of the protein ligands to the metal as well as their bond distances are still unknown. Spectroscopic data on the oxidized inactive enzyme would rule out the presence of cysteines and/or tyrosines because the electronic absorption spectra lack of the charge transfer bands characteristic of the interaction with such groups. Consequently, possible candidates for iron(II) coordination are histidines and carboxylates groups from aspartate and/or glutamate residues.

In order to shed some more light on the structure and the binding properties of the catalytic site, we decided to perform an X-ray absorption spectroscopic investigation on the native and on the adduct with 2-chlorophenol.

MATERIALS AND METHODS

Sample Preparation. Catechol 2,3-dioxygenase has been purified to homogeneity by using the procedure reported by Nakai et al. (1983), with the modifications suggested by

* Author to whom correspondence should be addressed.
‡ Università di Firenze.
§ Università di Siena.
∥ EMBL Outstation.
® Abstract published in *Advance ACS Abstracts,* July 1, 1994.

0006-2960/94/0433-10777$04.50/0

Arciero et al. (1985). The final specific activity was always higher than 300 units/mg. The enzyme was stored at 4 °C in degassed 50 mM phosphate buffer, pH 7.5, containing 10% acetone for more than 2 weeks without any loss of activity.

Samples for the XAS measurements were taken from the above solution concentrated under nitrogen to about 1.5 mM Fe(II) (sample 1) and introduced into 1-mm thick plastic cells (200 μL) covered with kapton windows. The 2-chlorophenol–enzyme complex sample (sample 2) was prepared by adding a 200-fold molar excess of inhibitor to the enzyme solution. In order to check the spectral reproducibility, two other samples were used later for a second experiment. Both were obtained from an independent preparation of the enzyme. One contained the native enzyme 2 mM Fe(II) (sample 3), and the other solution was equimolar in enzyme and 55 mM in the 2-chlorophenol inhibitor (sample 4). In the presence of such amounts of the ligand, all of the enzyme is converted to the adduct (K_i 2-chlorophenol = 5×10^{-4} M). The addition of the inhibitors did not affect the pH of the solution nor the protein stability.

XAS Measurements. X-ray absorption measurements on the enzyme samples were conducted at the EMBL EXAFS beamline (c/o DESY, Hamburg) (Hermes et al., 1984; Pettifer & Hermes, 1986). During data collection the synchrotron was operating at 4.5 GeV in dedicated mode with ring currents ranging from 45 to 15 mA. A Si(111) double crystal monochromator with an energy resolution of 1.8 eV at 7250 eV resulting in a $\Delta E/E = 2.5 \times 10^{-4}$ was used. The second monochromator crystal was detuned to 70% in order to reject higher order harmonics. The monochromator angle was converted to an absolute energy scale by utilizing a calibration technique (Pettifer & Hermes, 1985).

The protein XAS spectra were recorded by monitoring the X-ray fluorescence of the sample with a 13-element Ge solid-state detector. Data were collected at the iron edge (7122.7 eV at the edge jump inflection point for all samples). A series of 40–48 spectra were taken for each sample 1 and 2 at 20 K. The low temperature is used to reduce the signal attenuation due to the atomic thermal motion and to stabilize the samples toward irradiation (Chance et al., 1980; Powers, 1982). The spectra were recorded from 6912 to 7812 eV with variable step widths. In the XANES and EXAFS regions steps of 0.3 and 0.5–1.2 eV, respectively, were used. No evident damage of the protein samples occurred during the exposure to the X-ray beam as far as it can be judged by the constancy of the edge position and of the EXAFS oscillations observed between the first and the last collected XAS spectra. The data sets on samples 3 and 4 consisted of 25 and 28 spectra, respectively, taken using data collection parameters identical to those of samples 1 and 2.

Data Analysis. The data reduction based on standard methods (Teo, 1985; Scott, 1985) was performed by using the local set of programs EXPROG (Nolting & Hermes, 1992). The monochromator position was converted to absolute energy (see above). For each sample the scans were inspected for edge consistency, normalized by the edge jump, and averaged. The pre-edge peak areas were calculated by subtracting an arctangent function (fitted from 7108 to 7119 eV) from the normalized edge spectra and integrating over a range of ca. 10 eV (7108–7119 eV). The EXAFS spectrum was extracted by subtracting the slowly varying atomic background fitted with a multiknots cubic spline. The raw EXAFS was converted to k space and weighted by k^3 in order to compensate for the smaller amplitude at high k due to the decay of the photoelectron wave. The analysis of the EXAFS spectra utilizing rapid curved single and multiple scattering theory (Ashley & Doniach, 1975; Lee & Pendry, 1975; Teo, 1985; Gourman et al., 1984, 1986) was accomplished with the set of programs EXCURVE88 (Binsted et al.. 1988). The experimental spectrum has been matched with the theoretical simulation by adjusting the parameter ΔE_0, consequently the position of the peaks in the Fourier transform is approximately corrected for the phase shift. The values obtained were 12.9 and 16.0 eV for the enzyme samples 1 and 2, respectively; as a consequence $k = 1.84$ and 2.05 Å^{-1} represent the experimental absorption edges. These values were kept fixed in all subsequent curve fitting. The amplitude reduction factor was also fixed at 0.8 for all fits of both samples.[1] Fourier transforms were calculated in the k range 3.0–11.0 Å^{-1}. A Gaussian function was applied to the outer 0.1 Å of both sides of the window in order to provide a smooth termination of the Fourier back-transformed data. The distance ranges used in the back-transform are listed in the figures and tables captions.

In the EXAFS analysis of filtered data the number of independent points is approximately given by $2\Delta k \Delta R/\pi$ (Lee et al., 1981; Powers, 1982; Teo, 1985); hence for data between 3 and 11 Å^{-1} and a filtering window 1.1 Å wide like that used for the first neighbors analysis, we obtain 5.5 degrees of freedom, allowing us to use a maximum of five variable parameters. Consequently, only the distance and the Debye–Waller factor for each coordination shell were allowed to vary, whereas the coordination numbers were kept fixed. In the two- and multishell fits the E_0 values optimized for the first shell–single distance fit were used. The quality of the fit obtained was assessed by the fit index (FI) as defined within EXCURVE88:

$$\mathrm{FI} = \sum_i [(\chi^{(i)}_o - \chi^{(i)}_c)k^3]^2/n \times 100$$

where $\chi^{(i)}_o - \chi^{(i)}_c$ is the residual of point i, k is the value of the wave number at point i, and n is the number of experimental points.

Multiple scattering calculations were performed within EXCURVE88 and applied to the imidazole ligands. The constrained refinement approach has been used for the multiple shell fits (Binsted et al., 1992). The imidazole rings have been refined as rigid groups with the Fe–N distance fixed at the value obtained from the first shell analysis, only the value of the Fe–N–C angle has been allowed to vary. The ring interatomic distances have been taken from Orpen et al. (1989). Individual Debye–Waller parameters have been refined for the imidazole atoms. As a result a total of six parameters are used to describe the contribution to the EXAFS of the imidazoles.

RESULTS

Edge Data. Figure 1 shows the normalized XANES spectra of native and inhibited catechol 2,3-dioxygenase and of some iron model compounds (Nolting, 1985; Priggemeyer, 1991). It can be noticed that the edge position remains unchanged upon interaction with the 2-chlorophenol inhibitor. A comparison with the edge positions of Fe(II) and Fe(III) model compounds shows that the iron oxidation state is +2 for both enzyme samples.

[1] The parameter AFAC in EXCURVE88 represents the energy-independent amplitude factor introduced to compensate the reduction in amplitude due to multiple excitations. This corresponds to the $S(k)$ factor in the standard EXAFS formula, and it is usually between 0.7 and 0.9 (Teo, 1985).

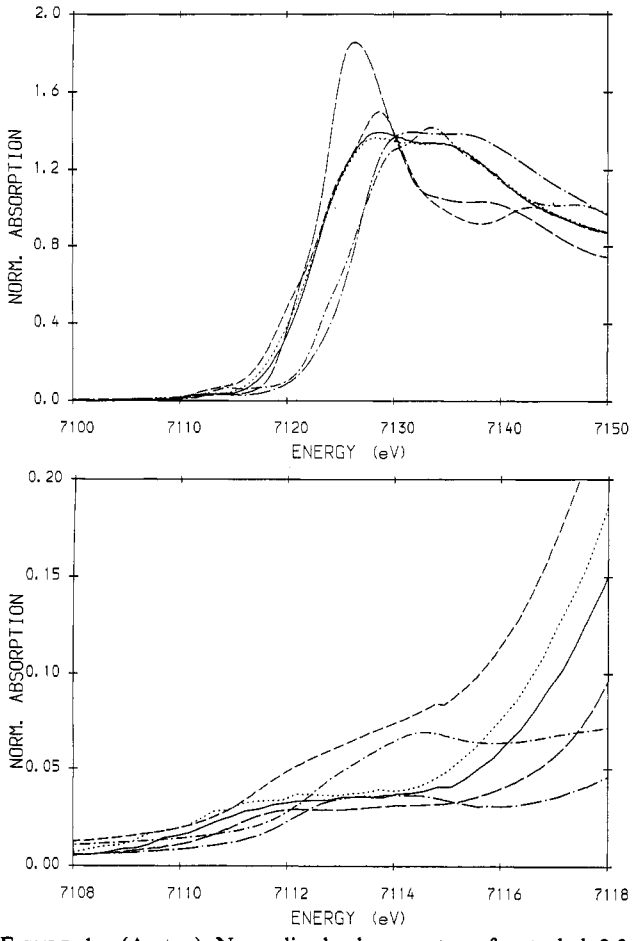

FIGURE 1: (A, top) Normalized edge spectra of catechol 2,3-dioxygenase samples and iron model compounds: native catechol 2,3-dioxygenase (—); inhibited catechol 2,3-dioxygenase (···); FeO (- - -); $(NH4)_2Fe(SO_4)_2{\cdot}6H_2O$ (– – –); Fe_2O_3 (- · -); $Fe(acac)_3$ (– · –). (B, bottom) Enlargement of the pre-edge region with the 1s–3d transition peaks of the catechol 2,3-dioxygenase samples and of the iron model compound. Lines are coded as in panel A.

A quantitative analysis of the pre-edge peak intensity can be performed in order to obtain information about the coordination geometry of the metal binding site. The pre-edge absorption feature is usually assigned to the 1s–3d transition in iron K-edge spectra (Shulman et al., 1976; Roe et al., 1984). According to spectral selection rules, this transition is forbidden, but its presence may be interpreted in terms of quadrupole and symmetry breaking effects. From X-ray absorption edge studies on Fe model compounds it was shown that the intensity of the pre-edge peak is within a characteristic range for each coordination geometry (Roe et al., 1984; Priggemeyer, 1991). Four Fe(II) model compounds with octahedral geometry were investigated to get typical values of 1s–3d peak intensities for ferrous coordination sites. The normalized pre-edge peak intensities observed for FeO, $(NH_4)_2FeSO_4{\cdot}6H_2O$, Fe(1,10-phenanthroline)$_3^{2+}$, and $K_4[Fe(CN)_6]{\cdot}3H_2O$ are 0.048, 0.044, 0.071, and 0.026 eV, respectively. This results in a typical range of 0.03–0.07 eV for octahedral Fe(II) environments. For comparison, recently reported pre-edge peaks of five-coordinate Fe(II) model compounds range from 0.089 to 0.107 eV (Randall et al., 1993). The pre-edge peak intensities derived from the XANES spectra of the native and the inhibited catechol 2,3-dioxygenase are 0.058 and 0.053 eV, respectively. Such values are consistent with an octahedral binding site in the native and in the inhibited form of catechol 2,3-dioxygenase. The present pre-edge data conflict with the electronic absorption data which indicate low symmetry and possibly five coordination (Mabrouk et al., 1991).

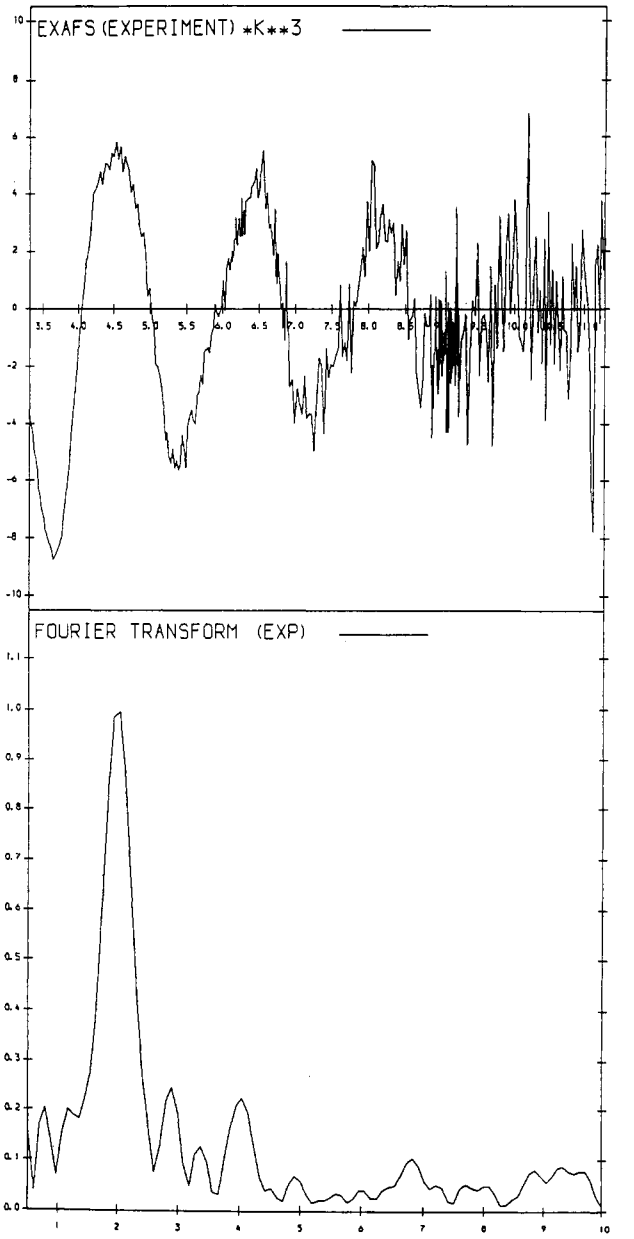

FIGURE 2: Experimental k^3 weighted EXAFS spectrum and its Fourier transform for the native catechol 2,3-dioxygenase enzyme.

The edge spectra of native and inhibited catechol 2,3-dioxygenase are very similar but not completely identical. In particular the intensity ratio of the two main peaks in the XANES spectra (at about 8 and 14 eV from the edge) changes upon interaction with 2-chlorophenol (see Figure 1).

EXAFS Data. Figures 2 and 3 show the k^3 weighted EXAFS spectra of samples 1 and 2, respectively, together with their Fourier transform. Due to the noise present at high k values, the spectra were truncated at $k = 11.0$ Å^{-1}. The presence of outer-shell peaks in the FT of native and inhibited catechol 2,3-dioxygenase suggests that histidine imidazoles are coordinated to the Fe(II) ions. Visual inspection of the two figures shows that upon addition of the inhibitor both the EXAFS and the FT are changed. In the FT of the 2-chlorophenol derivative the second shell peak is clearly enhanced with respect to the corresponding peak in Figure 2 and two outer shell peaks appear at ~3.7 and 4.2 Å instead of the single peak at 4.0 Å present in the FT of the native

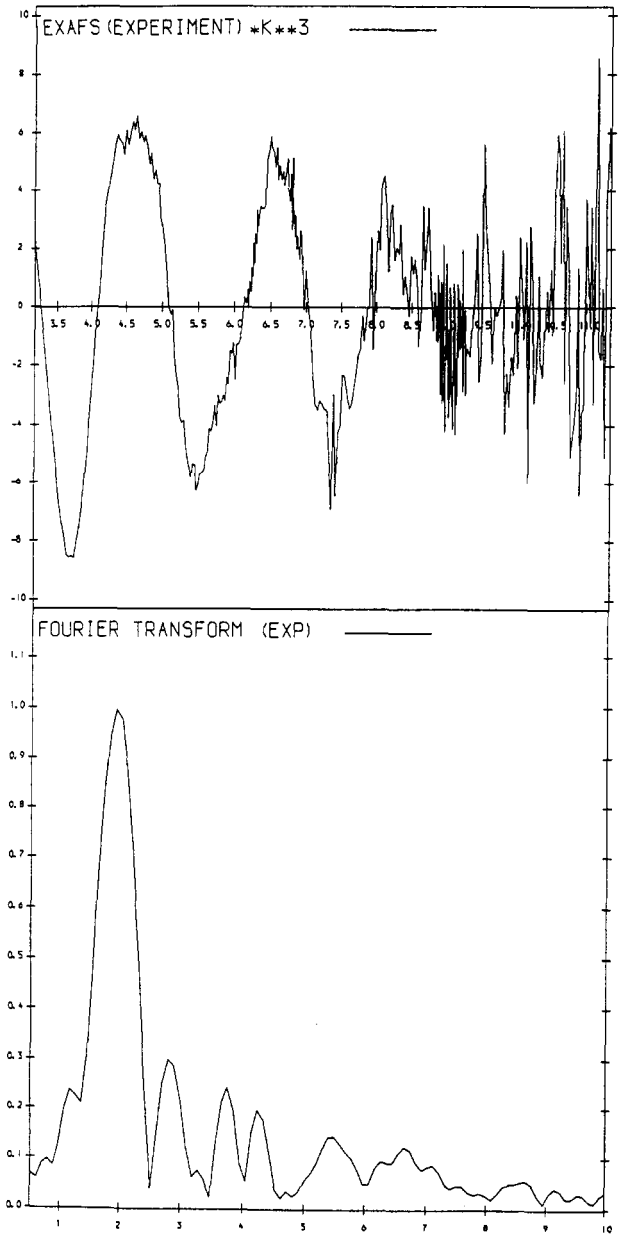

FIGURE 3: Experimental k^3 weighted EXAFS spectrum and its Fourier transform for the 2-chlorophenol–catechol 2,3-dioxygenase enzyme complex.

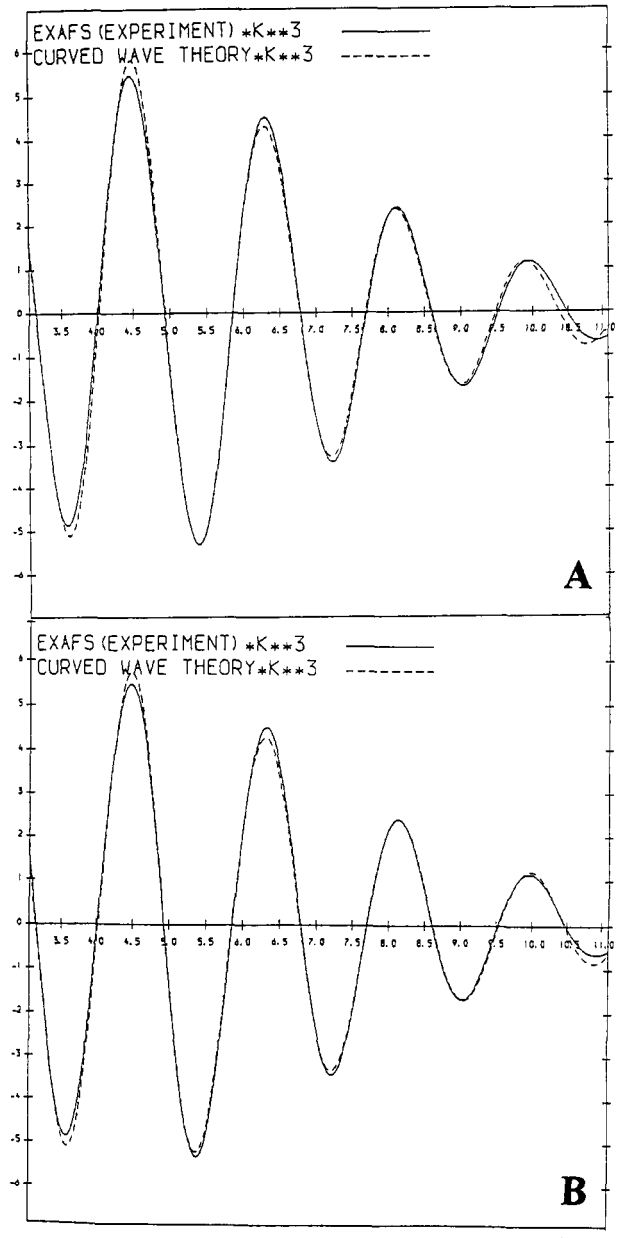

FIGURE 4: Experimental (—) and calculated (- - -) k^3 weighted filtered (between 1.0 and 2.1 Å) EXAFS spectra for the native catechol 2,3-dioxygenase enzyme. The calculated spectra are the result of the best single distance fit [FI = 0.10 (A)], and best two distances fit [FI = 0.05 (B)].

enzyme. These peaks are always present in the same position and with the same height both in the native and inhibited enzyme spectra when the FT is calculated over different k ranges (3–3.5 to 9.5–11 Å^{-1}). This fact indicates that these features are real and not dominated by the noise. The interaction with the 2-chlorophenol inhibitor causes only slight changes in the iron first coordination sphere.

First Shell Analysis. The first coordination shell contribution to the EXAFS for the two samples has been analyzed by Fourier filtering and back-transforming the FT between 1.0 and 2.1 Å (Figures 4 and 5). The dampening of the EXAFS oscillations at high k values is indicative of a wide range of bond distances among the iron first neighbors.

The simulations were first carried out with six, five, or four nitrogen/oxygen atoms at the same distance. A satisfactory result was obtained with five or six N/O atoms at 2.04–2.05 Å for sample 1 with the fit index FI = 0.15 and 0.10, respectively. A similar level of agreement could not be obtained with sample 2. For example, the best fit was achieved with six N/O at 2.03 Å and a FI = 0.58. The results of such fits are shown in Figures 4 and 5. It must be noticed that the single distance fits always resulted in quite large Debye–Waller factors, $2\sigma^2 = 0.022$ Å^2 (sample 1) and $2\sigma^2 = 0.021$ Å^2 (sample 2), suggesting a large spread of distances within this shell. Therefore two distances fits were attempted. The inclusion of the second ligand shell caused the dropping of the fit index from 0.10 to 0.05 and from 0.58 to 0.19 for sample 1 and 2, respectively. All the possible combinations of oxygen and nitrogen atoms summing up to six or five were attempted. The best results were obtained for both samples with the 4O–2N combination, although the 3O–3N and 3O–2N gave comparable fits. Statistical significance tests (Joyner et al., 1987) indicate that the 4O–2N ligand set is indistinguishable from the 3O–3N set. The results of the best fits are reported in Table 1 and in Figures 4 and 5 for sample 1 and 2, respectively. The first shells amplitudes of the two samples have been compared also by the ratio method (Stern et al., 1975) in order to obtain an independent estimate of the eventual

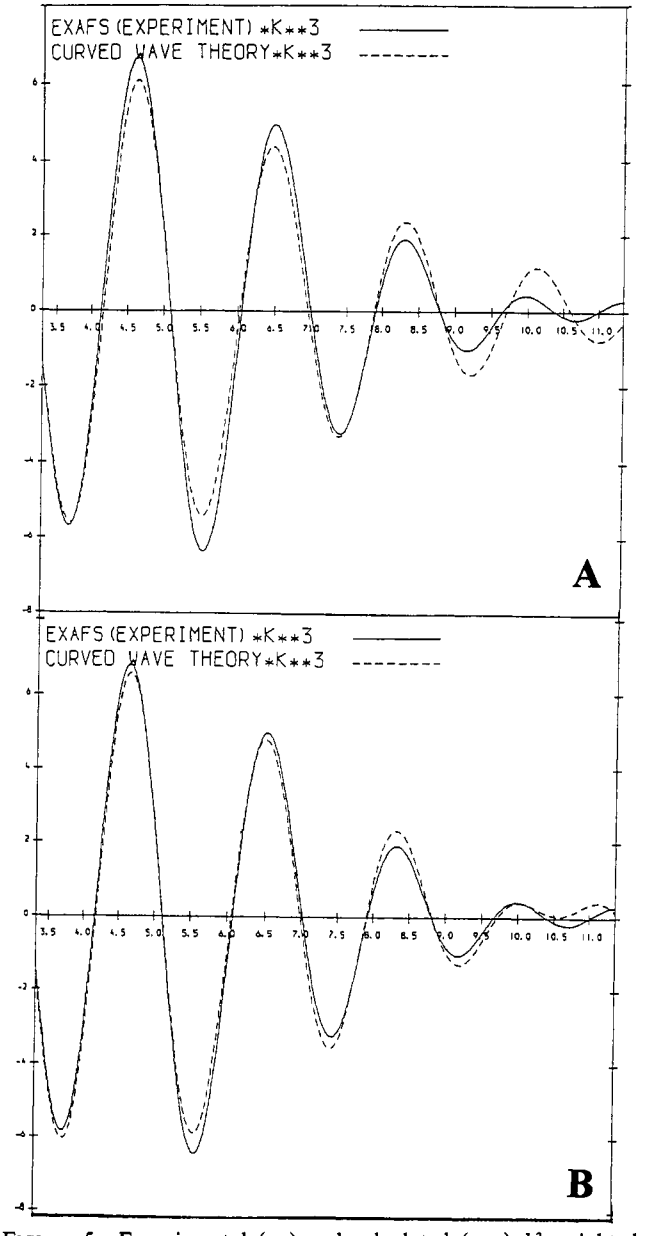

FIGURE 5: Experimental (—) and calculated (- - -) k^3 weighted filtered (between 1.0 and 2.1 Å) EXAFS spectra for the 2-chlorophenol inhibited catechol 2,3-dioxygenase enzyme. The calculated spectra are the result of the best single distance fit [FI = 0.58 (A)], and best two distances fit [FI = 0.19 (B)].

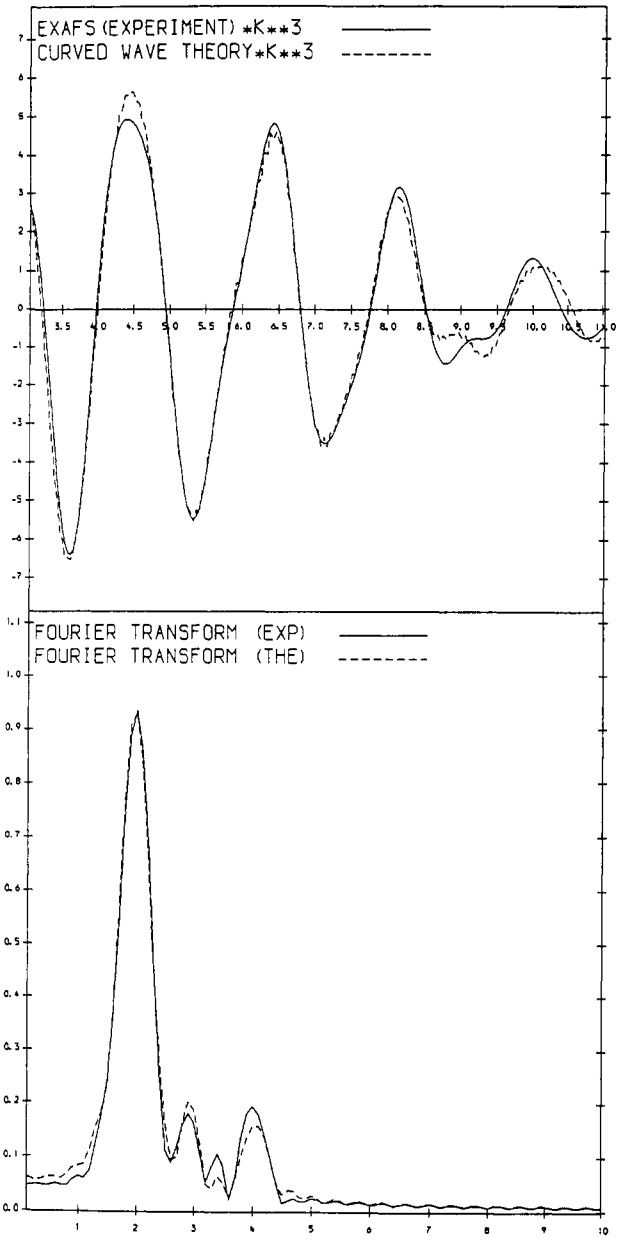

FIGURE 6: Experimental (—) and calculated (- - -) k^3 weighted filtered (between 1.0 and 4.1 Å) EXAFS spectra and their Fourier transform for the native catechol 2,3-dioxygenase enzyme. FI = 0.26.

differences between the two samples. The good linear dependence obtained for the ratio ln A_1/A_2 vs k^2 (where A_1 and A_2 are the amplitude functions of the native and inhibited enzyme, respectively) in the range 20–100 Å^{-2} and the intercept at 0.04 confirm that the two samples have iron first coordination shells composed of the same number of similar atoms (N/O).

Outer Shell Analysis. Due to the noise present in the experimental spectrum, the analysis of the outer shell ligands of the native catechol 2,3-dioxygenase iron ion was performed on Fourier filtered data from 1.0 to 4.1 Å as shown in Figure 6. The presence of the outer peaks in the FT is indicative of the presence of histidine residues in the Fe(II) coordination. We have attempted to quantitatively simulate these peaks by using multiple scattering calculations (Gourman et al., 1986) coupled to constrained refinement. Such an approach has been proven to be able to account for these features both for protein and model compound data (Bunker et al., 1982; Pettifer et al., 1986; Knowles et al., 1989; Hasnain & Strange, 1990; Binsted et al., 1992). Figure 6 shows that the main features of the catechol 2,3-dioxygenase spectrum and of its transform could be quite accurately reproduced by introducing in the simulation all the atoms of two imidazole rings coordinated at 2.17 Å in addition to the other first shell atoms. However, in order to simulate the peak at ~2.9 Å in the FT (Figures 1 and 6), it was necessary to introduce a further shell of 2.0 carbon atoms at 2.94 Å. The addition of these scatterers must be taken with caution because the peak at 2.9 Å may be due at least partially to noise and to Fourier series truncation effects. However, the distance of these atoms is consistent with that expected for the carbon atoms from iron-bound monodentate carboxylate groups. Further attempts were made to simulate the data with contributions from one or three imidazole groups, using the corresponding distribution of first shell N or O ligands: The results were not satisfactory, FI = 1.92 and 1.52 were, respectively, obtained for the two above reported cases.

The analysis of the inhibited enzyme spectrum shows that the first shell distances are only slightly affected by the

Table 1: One and Two Distance Fits of the First Fe(II) Iron Coordination Shell of Native and 2-Chlorophenol Inhibited Catechol 2,3-Dioxygenase[a]

native catechol 2,3-dioxygenase					catechol 2,3-dioxygenase–2Cl–phenol complex				
shell 1	shell 2	R (Å)	$2\sigma^2$ (Å^2)	FI	shell 1	shell 2	R (Å)	$2\sigma^2$ (Å^2)	FI
6O/N		2.05	0.022	0.10	6O/N		2.03	0.021	0.58
5O/N		2.04	0.018	0.15	5O/N		2.03	0.017	1.12
4O/N		2.04	0.013	0.56	4O/N		2.03	0.014	2.18
4O		2.02	0.014	0.05	4O		1.97	0.011	0.19
	2N	2.17	0.015			2N	2.14	0.004	
3O		2.01	0.017	0.07	3O		1.96	0.006	0.22
	3N	2.17	0.015			3N	2.13	0.003	
3O		2.01	0.007	0.09	3O		1.96	0.004	0.44
	2N	2.17	0.004			2N	2.13	0.003	

[a] E.s.d. on distances = ±0.02 Å.

interaction of the enzyme with 2-chlorophenol, whereas remarkable changes are apparent in the outer shells that are consistent (together with the change in the XANES peaks) with the direct binding of the inhibitor to the metal ion. Assuming the monodentate binding of the inhibitor through the phenolate oxygen, the phenol ring should not contribute to multiple scattering effects being tilted of about 110–120° with respect to the Fe–O bond and the torsion angle Fe–O–C1(phenol)–C2(phenol) being somewhere between 100° and 120° (i.e., Fe, O, C1, and C2 are not in the same plane) as observed in the crystal structures of Fe(III)–phenolate complexes (Koch & Millar, 1982) and of the protein lactoferrin (Anderson et al., 1989). Indeed such a model added to the multiple scattering contributions from two imidazole rings at 2.17 Å from iron was able to reproduce all the features of the EXAFS spectrum and of its FT. This model comprises a chlorine atom at 4.26 Å and a further shell of two carbon atoms at 3.82 Å which may account for the phenolate C2 and C6 carbons. The contribution from the C1 phenolate carbon is expected at about 3.2 Å, and it is superimposed with the imidazole C2–C5 shells. Figure 7 shows the results of this simulation with the best-fit parameters reported in Table 2. The peak at 4.2 Å bears contributions from the outer imidazole shells and the putative chlorine atom. As a matter of fact the contributions from chlorine and carbon atoms at that distance are out of phase. For this reason adding the chlorine shell has the effect to improve the fit (FI goes from 0.60 to 0.56) by slightly dampening the height of the outermost peak. Even though the statistical analysis indicates that such improvement is significant, this cannot be taken as an experimental proof of the detection of a chlorine atom at that distance. It simply means that our model of monodentate binding of the inhibitor is consistent with the experimental data.

^{1}H NMR data on *o*-chlorophenol were collected in order to obtain independent information on the inhibitor–enzyme complex. The spectrum of the inhibitor consists in a series of very narrow multiplets spanning from 6.6 to 7.4 ppm from TMS. Upon addition of the enzyme in the 1:100 iron(II) active site/inhibitor ratio, the spectrum shows four broad signals with T_1 ranging from 0.28 to 0.40 s. T_{1M}^{-1} paramagnetic enhancements to the relaxation rates ranging from 230 to 340 s^{-1} are perfectly consistent with direct binding of the phenol to the paramagnetic center, the nuclear relaxation mechanisms being both dipolar and ligand centered in origin (Bertini & Luchinat, 1986). Analogous values were obtained in the case of the *o*-methoxy phenol (Bertini et al., 1994). Also, the changes observed in the fine structure of the NMR spectra of the bound inhibitor with respect to the free one are consistent with the direct binding of the ligand to the paramagnetic center.

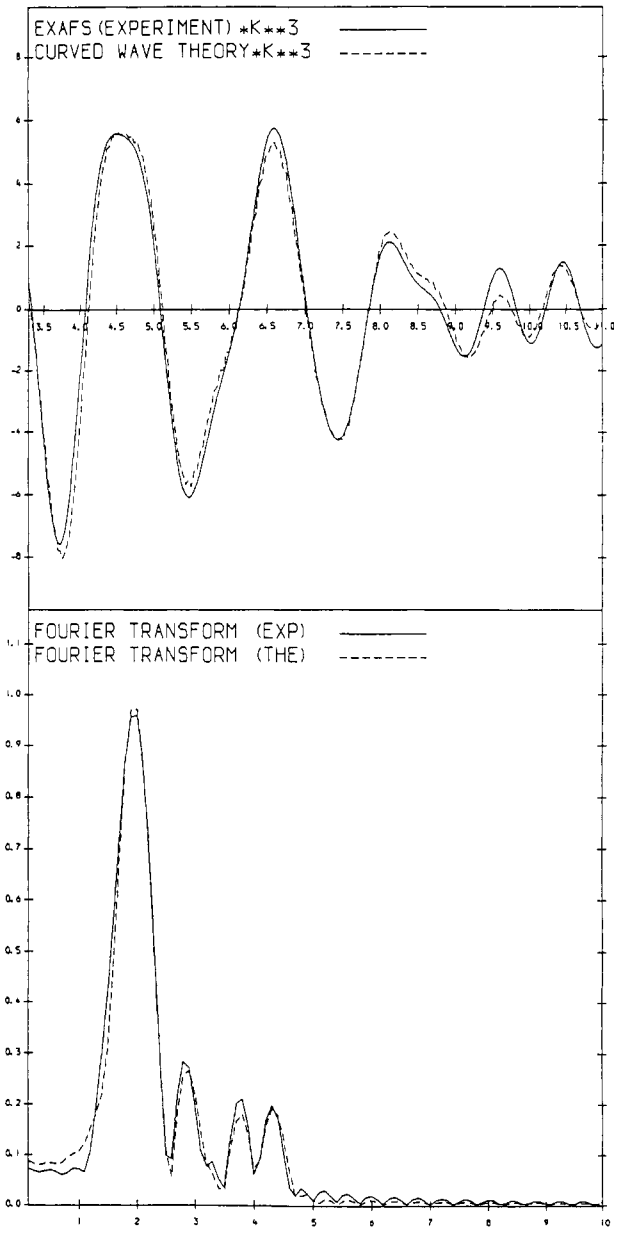

FIGURE 7: Experimental (—) and calculated (- - -) k^3 weighted filtered (between 1.0 and 4.1 Å) EXAFS spectra and their Fourier transform for the 2-chlorophenol–catechol 2,3-dioxygenase enzyme complex. FI = 0.56.

DISCUSSION

Analyzing EXAFS data from protein samples is always complicated by a series of problems (Lee et al., 1981; Powers, 1982; Cramer, 1987). The quality of the data is poor due to

Table 2: Parameters Used To Simulate the Fourier Filtered (1.0–4.1 Å) Data of Samples 1 and 2 As Reported in the Figures[a]

native catechol 2,3-dioxygenase (FI = 0.26)			catechol 2,3-dioxygenase–2Cl-phenol complex (FI = 0.56)		
shell	R (Å)	$2\sigma^2$ (Å)^2	shell	R (Å)	$2\sigma^2$ (Å)^2
4O	2.02	0.012	4O	1.97	0.011
*2N	2.17	0.008	*2N	2.14	0.002
2C	2.94	0.016	2C	2.90	0.004
*2C	3.06	0.016	*2C	3.04	0.012
*2C	3.28	0.006	*2C	3.28	0.014
*2N	4.23	0.006	2C	3.82	0.006
*2C	4.32	0.013	*2N	4.24	0.011
			1Cl	4.26	0.015
			*2C	4.33	0.012

[a] E.s.d. on distance = ±0.02 Å. The asterisk refers to the atomic shells describing the imidazole groups. The Fe–N1(Imid)–C2 (Imid) angles for native and inhibited catechol 2,3-dioxygenase refined to 132° and 135°, respectively.

the dilution of the metal investigated in the biological matrix with consequent limitation of the data range available and distance resolution. Furthermore, the intrinsic complexity of a system with a high static disorder and containing different ligand types requires a high number of parameters to be described. High correlations are present between different shells of atoms thus biasing the singleness of the least-squares minimum: as a consequence, the determination of the parameters, especially the coordination number, becomes less accurate.

However, from the results of the analysis outlined above, it is possible to obtain further hints about the structure of the active site of catechol 2,3-dioxygenase and draw some inference about the inhibition mechanism of 2-chlorophenol.

The position of the edge with the inflection point at 7122.7 eV is constant for both samples indicating the presence of Fe(II) ions. The analysis of the pre-edge 1s–3d transition peak indicates that the coordination geometry is octahedral for both the native and the inhibited enzyme rather than five coordinate. Our analysis is founded only on four octahedral and two published pentacoordinated Fe(II) model compounds of known structure which are obviously insufficient to establish ranges of 1s–3d peak areas characteristic of each coordination geometry. However, the very low value for the pre-edge peak area from our experiments seems not to be consistent with a noncentrosymmetric environment like the square-pyramidal or trigonal-bipyramidal pentacoordination of the ferrous ion. Similar conclusions have been drawn for proteins containing the iron atom in a distorted octahedral environment like non-heme iron(III) dioxygenases (Roe et al., 1984), hemerythrin (Elam et al., 1982), acid phosphatase (Kauzlarich et al., 1986), and isopenicillin N synthase (Randall et al., 1993; Scott et al., 1992). However, low symmetry components and/or monobidentate behavior of carboxylate groups could complicate the analysis.

Although the difference between five- and six-coordination is within the experimental error for EXAFS protein data, it has to be noticed that both the one-shell and the two-shell fits of the nearest Fe(II) neighbors give low FI for the six coordination.

If six coordination is assumed, the first iron coordination shell would appear to be made of six N/O ligands at an average distance of 2.05 Å. However, the first neighbors contribution to the EXAFS is better simulated by two shells of light atoms at 2.02 and 2.17 Å. Both the 2.05 and 2.02 Å distances are quite short for octahedral Fe(II) compounds; however, it may be noticed that the distances between 1.998 and 2.062 Å have been reported for Fe(II)–O (carboxylate) bonds in model compound crystal structures (Borovik et al., 1990; Martinez-Lorente et al., 1991; Rakotonandrasana et al., 1991; Tolman et al., 1991; Chiou & Que, 1992; Ménage et al., 1992; Zang et al., 1993). The Fe(II)–N distances of 2.17 Å are characteristic of Fe(II)–N(aromatic) bonds, and similar distances have been measured from EXAFS of isopenicillin N synthase (Scott et al., 1992). The outer shell analysis gives evidence of the presence of histidines in the coordination sphere. The quantitative analysis tends to favor two histidines. Trials to fit the spectrum with contributions from one or three imidazole groups were less satisfactory. The EXAFS data can be reasonably well reproduced also with five atoms in the first coordination shell. The nearest neighbor shell could be simulated with three oxygens at 2.02 Å and two nitrogens at 2.17 Å from the metal. This is not surprising because the difference between six and five coordination is within the usual 20–25% error on the estimate of coordination numbers from protein EXAFS data (Cramer, 1987). Indeed a square-pyramidal pentacoordination for catechol 2,3-dioxygenase has been proposed from the analysis of absorption, circular dicroism, and magnetic circular dicroism spectroscopies (Mabrouk et al., 1991). The nature of the remaining ligands remains of course speculative. The oxygen donors are probably provided by aspartate or glutamate carboxyl groups. The presence of at least a water molecule was observed through EPR experiments on NO derivatives (Arciero et al., 1985). Independent spectroscopic observations have ruled out the participation of tyrosinate ligands (Lipscomb & Orville, 1992). The present study suggests that most probably there are at least two histidine ligands; hence it is reasonable that one or two further protein ligands are present in the first coordination sphere of the iron ion, the substrates probably removing water molecules. As suggested by EPR studies on the nitrosyl–enzyme complex (Arciero et al., 1985), when the enzyme is working, three iron coordination sites are occupied by the substrates. Scheme 2 reports the active site of native (A) and 2-chlorophenol inhibited catechol 2,3-dioxygenase (B) as determined from our data (the relative positions of the histidine residues are only schematic, and L means N/O donors). From the slight intensity changes of the main edge XANES peaks and from the first shell fitting of sample 2, it can be concluded that the arrangement of ligands is somewhat different between the two samples.

Scheme 2

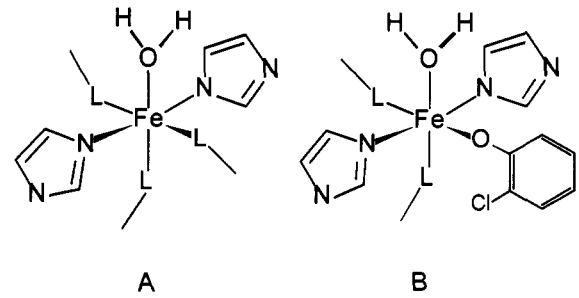

A B

The difference between the first shell distances obtained for the inhibited with respect to the native enzyme are at most within 2 e.s.d. and hence are barely significant. However, the worse fits obtained in every case for sample 2 seem to indicate that two distances are not enough to describe the first coordination shell of the complex.

The constancy of the first shell coordination observed upon inhibitor addition is in agreement with Mössbauer data which show that no detectable changes occur upon catechol binding

to the active site iron(II) ion of catechol 2,3-dioxygenase (Tatsuno et al., 1980).

The perturbations observed in the EXAFS spectrum upon addition of the 2-chlorophenol inhibitor result mostly from an outer sphere ligand rearrangement of the iron atom. The outer shell analysis of the 2-chlorophenol inhibited sample shows a binding mode of the inhibitor which is consistent with our NMR data analysis (Bertini et al., 1994). The overall picture indicates that the inhibitor molecule is directly bound to the metal replacing one of the donor atoms of the native enzyme. The outer shell simulation reported in Figure 7 suggests that the histidine residues are still coordinated to the Fe(II) ion in the inhibited enzyme.

ACKNOWLEDGMENT

The authors acknowledge the use of technical facilities within the laboratories of the MASIMO network and the European Union Human Capital and Mobility Grant ER-BCHRXCT920072.

REFERENCES

Anderson, B. F., Baker, H. M., Norris, G. E., Rice, D. W., & Baker, E. N. (1989) *J. Mol. Biol. 209*, 711–734.

Arciero, D. M., & Lipscomb, J. D. (1986) *J. Biol. Chem. 261*, 2170–2178.

Arciero, D. M., Lipscomb, J. D., Huynh, B. H., Kent, T. A., & Münck, E. (1983) *J. Biol. Chem. 258*, 14981–14991.

Arciero, D. M., Orville, A. M., & Lipscomb, J. D. (1985) *J. Biol. Chem. 260*, 14035–14044.

Ashley, C. A., & Doniach, S. (1975) *Phys. Rev. B 11*, 1279–1288.

Bertini I., & Luchinat, C. (1986) *NMR of Paramagnetic Molecules in Biological Systems*, Benjamin/Cummings, Menlo Park, CA.

Bertini, I., Briganti, F., & Scozzafava, A. (1994) *FEBS Lett. 343*, 56–60.

Binsted, N., Gurman, S. J., & Campbell, J. W. (1988) SERC Daresbury Laboratory Program, Daresbury Laboratory, Warrington, U.K.

Binsted, N., Strange, R. W., & Hasnain, S. S. (1992) *Biochemistry 31*, 12117–12125.

Borovik, A. S., Hendrich, M. P., Holman, T. R., Münk, E., Papaefthymiou, V., & Que, L., Jr. (1990) *J. Am. Chem. Soc. 112*, 6031–6038.

Bunker, G., Stern, E. A., Blakenship, R. E., & Parson, W. W. (1982) *Biophys. J. 37*, 539–551.

Chance, B., Angiolillo, P., Yang, E. K., Powers, L. (1980) *FEBS Lett. 112*, 178–182.

Chiou, Y., & Que, L., Jr. (1992) *J. Am. Chem. Soc. 114*, 7567–7568.

Cramer, S. (1987) in *X-ray Absorption, Principles, Applications, Techniques of EXAFS, SEXAFS and XANES* (Kronings-berger, D. C., & Prins, R., Eds.) Chapter 7, pp 257–320, Wiley Interscience, New York.

Elam, W. T., Stern, E. A., McCallum, J. D., & Sanders-Loehr, J. (1982) *J. Am. Chem. Soc. 104*, 6369–6373.

Gurman, S. J., Binsted, N., & Ross, I. (1984) *J. Phys. C: Solid State Physics 17*, 143–151.

Gurman, S. J., Binsted, N., & Ross, I. (1986) *J. Phys. C: Solid State Physics 19*, 1845–1861.

Harayama, S., & Timmis, K. N. (1992) in *Metal Ions in Biological Systems*, Vol. 28, Chapter 4, pp 99–156, Marcel Dekker Inc., New York.

Hasnain, S. S., & Strange, R. W. (1990) in *Biophysics and Synchrotron Radiation* (Hasnain, S. S., Ed.) p 104 Ellis Horwood Ltd., Chichester, U.K.

Hermes, C., Gilberg, E., & Koch, M. H. (1984) *J. Nucl. Instrum. Methods 222*, 207–214.

Hirata, F., Nakazawa, A., Nozaki, M., & Hayaishi, O. (1971) *J. Biol. Chem. 246*, 5882–5887.

Hori, K., Hashimoto, T., & Nozaki, M. (1973) *J. Biochem. (Tokyo) 74*, 375–384.

Joyner, R. W., Martin, K. J., & Meehan, P. (1987) *J. Phys. C: Solid State Physics 20*, 4005–4012.

Kauzlarich, S. M., Teo, B. K., Zirino, T., Burman, S., Davis, J. C., & Averill, B. A. (1986) *Inorg. Chem. 25*, 2781–2785.

Knowles, P. F., Strange, R. W., Blackburn, N. J., & Hasnain, S. S. (1989) *J. Am. Chem. Soc. 111*, 102–107.

Koch, S. A., & Millar, M. (1982) *J. Am. Chem. Soc. 104*, 5255–5257.

Kojima, Y., Itada, N., & Hayaishi, O. (1961) *J. Biol. Chem. 236*, 2223–2228.

Lee, P. A., & Pendry, J. B. (1975) *Phys. Rev. B 11*, 2795–2811.

Lee, P. A., Citrin, P. H., Eisenberger, P., & Kinkaid, B. M. (1981) *Rev. Mod. Phys. 53*, 769–807.

Lipscomb, J. D., & Orville, A. M. (1992) in *Metal Ions in Biological Systems*, Vol. 28, Chapter 8, pp 243–298, Marcel Dekker Inc., New York.

Mabrouk, P. A., Orville, A. M., Lipscomb, J. D., & Solomon, E. I. (1991) *J. Am. Chem. Soc. 113*, 4053–4061.

Martinez-Lorente, M. A., Tuchagues, J. P., Petruleas, V., Savariault, J. M., Poinsot, R., & Drillon, M. (1991) *Inorg. Chem. 30*, 3587–3589.

Ménage, S, Zang, Y., Hendrich, M. P., & Que, L., Jr. (1992) *J. Am. Chem. Soc. 114*, 7786–7792.

Nakai, C., Hori, K., Kagamiyama, H., Nakazawa, T., & Nozaki, M. (1983) *J. Biol. Chem. 258*, 2916–2922.

Nolting, H. F. (1985) Diploma Thesis, Westfälische Wilhelms-Universität zu Münster, Germany.

Nolting, H. F., & Hermes, C. (1992) EXPROG: EMBL EXAFS data analysis and evaluation program package for PC/AT, European Molecular Biology Laboratory, c/o DESY, Hamburg.

Nozaki, M., Kagamiyama, H., & Hayaishi, O. (1963) *Biochem. Z. 338*, 582–590.

Nozaki, M., Ono, K., Nakazawa, T., Kotani, S., & Hayaishi, O. (1968) *J. Biol. Chem. 243*, 2682–2690.

Orpen, A. G., Brammer, L., Allen, F. H., Kennard, O., Watson, D. G., & Taylor, R. (1989) *J. Chem. Soc., Dalton Trans. (Suppl.)*, S1–S83.

Pettifer, R. F., & Hermes, C. (1985) *J. Appl. Crystallogr. 18*, 404–412.

Pettifer, R. F., & Hermes, C. (1986) *J. Phys. C: Solid State Physics 8*, 127–133.

Pettifer, R. F., Foulis, D. L., & Hermes, C. (1986) *J. Phys. C: Solid State Physics 8*, 545–550.

Powers, L. (1982) *Biochim. Biophys. Acta 683*, 1–38.

Priggemeyer, S. (1991) Ph.D. Dissertation Thesis, Westfälischen Wilhelms-Universität zu Müster, Germany.

Que, L., Jr. (1989) in *Iron Carriers and Iron Proteins* (Loehr, T., Ed.) p 467–524, VCH, New York.

Rakotonandrasana, A., Boinnard, D., Savariault, J.-M., Tuchagues, J.-P., Petrouleas, V., Cartier, C., & Verdaguer, M. (1991) *Inorg. Chim. Acta 180*, 19–31.

Randall, C. R., Zang, Y., True, A. E., Que, L. Jr., Charnock, J. M., Garner, C. D., Fujishima, Y., Schofield, C. J., & Baldwin, J. E. (1993) *Biochemistry 32*, 6664–6673.

Roe, A. L., Schneider, D. J., Mayer, R. J., Pyrz, J. W., Widom, J., & Que, L., Jr. (1984) *J. Am. Chem. Soc. 106*, 1676–1681.

Scott, R. A. (1985) *Methods Enzymol. 111*, 414–459.

Scott, R. A., Wang, S., Eidsness, M. K., Kriauciunas, A., Frolik, C. A., & Chen, W. J. (1992) *Biochemistry 31*, 4596–4601.

Shulman, R. G., Yafet, Y., Eisenberger, P., & Blumberg, W. E. (1976) *Proc. Natl. Acad. Sci. U.S.A. 73*, 1384–1388.

Stern, E. A., Sayers, D. E., Lytke, F. W. (1975) *Phys. Rev. B 11*, 4836–4846.

Tatsuno, Y., Saeki, Y., Nozaki, M., Otsuka, S., & Maeda, Y. (1980) *FEBS Lett. 112*, 83–85.

Teo, B. K. (1985) in *EXAFS: Basic Principles and Data Analysis*, Inorganic Chemistry Concepts Vol. 9, Springer-Verlag, Berlin.

Tolman, W. B., Liu, S., Bentsen, J. G., & Lippard, S. J. (1991) *J. Am. Chem. Soc. 113*, 152–164.

Zang, Y., Elgren, T. E., Dong, Y., & Que, L., Jr. (1993) *J. Am. Chem. Soc.115*, 811–813.